Debris orbit prediction accuracy from orbit determinations using very short-arc optical and laser tracking data*

J. C. Bennett
The SPACE Research Centre, School of Mathematical and Geospatial Sciences, RMIT University, GPO Box 2476, Melbourne, Victoria, 3001, AUSTRALIA
EOS Space Systems Pty. Ltd., Mount Stromlo Observatory, Cotter Road, Weston Creek, Australian Capital Territory, 2611, AUSTRALIA
J. Sang
School of Geodesy and Geomatics, Wuhan University, 129 Luoyu Road, Wuhan, 430079, CHINA
C. Smith
EOS Space Systems Pty. Ltd., Mount Stromlo Observatory, Cotter Road, Weston Creek, Australian Capital Territory, 2611, AUSTRALIA
K. Zhang
The SPACE Research Centre, School of Mathematical and Geospatial Sciences, RMIT University, GPO Box 2476, Melbourne, Victoria, 3001, AUSTRALIA

ABSTRACT

In this paper results are presented from an orbit determination study fitting short-arc optical and laser tracking data from the Space Debris Tracking System located at Mount Stromlo, Australia.

Fifteen low-Earth orbit debris objects were considered in the study with perigee altitudes in the range 550–850 km. In most cases, a 2-day orbit determination was considered using 2 passes of optical and 2 passes of laser tracking data. A total of 68 orbit determinations were performed fitting 3-dimensioal observational data (angles and range) and orbit prediction residuals were calculated by comparing the orbit predictions with subsequent tracking data. A comparison was made between the orbit prediction accuracies for 2 orbit determination variants: (1) Entire passes (~2–3 minutes each) were fitted during the orbit determination process; (2) Only 5 seconds was fitted from the beginning of each pass.

Overall, the short-arc orbit determination results in (slightly) worse orbit predictions when compared to using the full observation arcs; however, the savings in tracking load outweighs the reduction in accuracy. If the optical data was left out of the short-arc orbit determination process (i.e., only fitting short-arc range observations) then most cases diverged. If the laser data was left out (i.e. only fitting short-arc angular observations) then the orbit prediction accuracy reduced significantly. This shows the importance of 3-dimenional positioning. Two-line element data was used to help constrain the orbit determination process in the 1-dimensional and 2-dimensional fitting, resulting in better convergence rates and improving the orbit prediction accuracy but failed to meet the accuracy of fitting 3-dimensional observational data.

The results have important implications for an optical and laser debris tracking network by reducing the tracking load.

1. INTRODUCTION

Due to the large number of objects, particularly in the low-Earth orbit (LEO) environment, providing reliable orbital information is a challenging task. The most comprehensive, publicly accessible source of orbital data is in the form of two-line element (TLE) sets available through Space-Track.org (www.space-track.org) which currently contains

* This paper is based on an article "An analysis of very short-arc orbit determination for low-Earth objects using sparse optical and laser tracking data" submitted to Advances in Space Research, under review.

data for over 17,000 on-orbit objects. Orbital information is imperative for space situational awareness, particularly for conjunction assessments. The requirement to routinely track potentially damaging, uncontrolled objects is a difficult task requiring international efforts to protect space assets and preserve space.

The debris laser tracking system located at EOS Space Systems on top of Mount Stromlo, Canberra, can track space debris using optical and laser tracking methods and delivers 3-dimensional observations. The system operation is limited to two terminator sessions per day due to the need for the debris target to be sun-illuminated and visible from the ground station. The azimuth and elevation data collected from the optical tracking system has been shown to have approximately 1.5 arc-second root-mean-square (RMS) error. The debris laser ranging system range accuracy is better than 1.5 metres RMS error [1, 2].

Optimally tasking the laser tracking station is a well-constrained problem involving pass duration, geometry, the number of objects to track, telescope slew time, etc. There are multiple ways to optimise an individual tracking session based on specific campaign needs, for example, different priority for different targets. If the requirement for the pass duration can be minimised, the number of objects that can be tracked during a session increases.

The focus here is to investigate the effects of reducing the tracking data used in an orbit determination (OD) procedure rather than optimising a tracking session operation. The goal is to reduce the tracking data requirements without too much loss of orbit prediction (OP) accuracy in a data sparse situation (i.e. 2 passes) for low LEO debris objects – where atmospheric drag effects are the dominant source of orbit perturbations. The authors have extensively investigated the OP accuracy achievable from an OD fitting sparse optical and laser tracking data [3-5]. This paper investigates the notion that fitting the full pass data adds little to the OP accuracy since the separation of the observation arcs (at least 24 hours in this paper) provides the dominant geometrical constraint to the OD and very short-arc observation arcs would suffice.

In what follows, the optical and laser tracking data distribution is presented, followed by a description the OD/OP analyses to determine:

(1) If accurate OPs result from fitting very short-arc 3D observational data collected on 2 nights;
(2) If so, whether accurate OPs result from fitting very short-arc 2D or 1D observations;
(3) Whether TLE data can be used to improve the cases where convergence is not achieved or OP accuracy is poor.

Then the results of the study are presented and finally some conclusions are drawn.

2. TRACKING DATA DISTRIBUTION

During April/May 2013, EOS Space Systems performed a debris laser tracking campaign targeting low-Earth orbit debris objects. Several objects were successfully tracked and the short-term OP accuracy generated by fitting this data as well as data from other campaigns can be found in [6]. The data distribution of the tracked objects selected for the short-arc analysis is shown in Table 1.

For each laser pass indicated by an asterisk, there was also an associated angular pass collected by the optical tracking system. Each of the angular and range observation full passes are ~2–3 minutes.

3. ORBIT DETERMINATION AND PREDICTION

Using the available tracking data from the April/May tracking campaign, a series of OD/OP computations are performed. The OD is set to contain tracking data from 2 nights with a maximum OD length set to 3 days. Most of the ODs are 2-days containing 2 passes. For example, Object 1430 was tracked on the 24th and 25th of April and an OD is set to start at beginning of the 24th of April (at midnight) and span 2 days. In this case there is data available for predictions for 1, 2, 6, and 7 days after the OD (neglecting OPs longer than 7 days). Similarly, Object 2125 was tracked on the 25th and 27th of April and an OD is set to start on the 25th of April and span 3 days. In this case there is data available for determining OP accuracy 4 and 5 days after the OD (neglecting OPs longer than 7 days), and so on. These two examples are shown in Table 1. This results in a total of 68 OD computations. The number of OD cases with data available for each OP prediction period is detailed in Table 2.

Table 1: Data distribution for the April/May 2013 tracking campaign. A "*" denotes a laser pass was collected on the associated date. The perigee and apogee are in km. Two of the 68 OD windows considered are indicated in red.

	April						**May**										
NORAD ID	**23**	**24**	**25**	**26**	**27**	**28**	**1**	**2**	**4**	**5**	**6**	**7**	**8**	**9**	**10**	**Perigee**	**Apogee**
1430		*	*	*	*		*	*		*	*		*		*	720	799
2125			*		*		*	*		*		**	*	*	*	596	821
2621	*	*	*			*		*		*	*				*	587	677
2980			*		*			*		*	*	*		*		628	772
5557		*		*	**			*	*	*			*		*	767	840
6275		*	*	*	*		*	*	*		*		*	*	*	775	828
8956		*	*		*	*	*	*	*	*	*			*		639	683
11060				*	*			*					*			824	841
13923		*				*	*	*	*	*	**	*			**	786	810
17122					*	*	*	*	*				*	*	*	663	676
23606			*	*	*	*	*		*	*			*		*	599	607
25475		*	**	*		*	**		*		*		*	*	*	787	791
26121	*	*	*				*		*	*	*		*	*		561	657
26702		*			*			*	*	*	*	*		*	*	565	571
26703				*	*				*	*			*	*	*	587	590

Table 2. The number of ODs with data available *x*-days after the end of the OD used to create the OP summary results.

OP period	**# of passes for OP RMS calculation**
1-day	33
2-day	26
3-day	25
4-day	25
5-day	22
6-day	20
7-day	16

A batch least squares OD fitting procedure is used with the Earth gravitational effect modelled using a EIGEN-GL05C gravity model [7], truncated to degree and order 100. The ocean tidal effects are included through the CSR 3.0 ocean tidal model [8], and the solid Earth tidal force is computed using the specification given in [9, Ch. 6]. Third body gravitational forces are computed using the DE200 planetary ephemeris. The area-to-mass ratio of the object is assumed to be $A/m = B_c/C_D = B_c/2.2$, where A is the unknown cross sectional area in the direction of motion in m^2, m is the mass in kg, also unknown, B_c is the object's ballistic coefficient estimated using the method in [10], and C_D is the drag coefficient (assumed to be 2.2 here). The B_c values are shown in Table 3 for the objects in Table 1. When computing the radiation pressure forces, the solar radiation pressure coefficient is fixed at 1.1 and the area-to-mass ratio is taken as A/m obtained above. The density model used is the NRLMSISE-00 model [11]. In each case the initial state for the OD process is provided by the first available TLE immediately before the OD window. Apart from the B_c, gathered from the long-term TLE data, no other object information is provided in the OD. It is also assumed that all of the objects are spherical.

Table 3: Ballistic coefficients determined from long term TLE data using the method described in [10].

NORAD ID	B_c (m^2/kg)
1430	0.017358
2125	0.020766
2621	0.013053
2980	0.021077
5557	0.032186
6275	0.044729
8956	0.039599
11060	0.029047
13923	0.027836
17122	0.048064
23606	0.035207
25475	0.107778
26121	0.038221
26702	0.025941
26703	0.015281

Two OD variants are considered to determine the reduction in OP accuracy when dealing with very short-arc observations:

(1) A least squares OD procedure is used to fit the full pass data;
(2) The OD process is repeated but with only 5 seconds of data from the beginning of each pass.

Three data scenarios are considered to investigate the change in OP accuracy when only optical (2-dimensional) or only range (1-dimensional) observations are available for the OD fitting. In each OD variant above the tracking data observations can be taken as:

(a) 1D – debris laser ranging (DLR) observations are considered only;
(b) 2D – optical angles observations are considered only; and,
(c) 3D – DLR and angles observations are both considered.

For example, an OD fitting 3D full pass data is denoted as OD variant (1c). Similarly, and OD fitting only 1D 5 second passes is denoted as OD variant (2a), and so on.

Obtaining reliable OPs from sparse tracking observations is difficult and in some cases the OD will diverge. In these circumstances other information is needed to provide reliable results. The TLE data sets are an excellent source of information and can be used to aid OD convergence. In the 1D and 2D data cases, convergence of the very short-arc ODs is assisted using TLE pseudo-observations generated using the SGP4 propagator [12] from TLEs that fall within the OD period. This leads to improved convergence rates and OP accuracy.

In the absence of "true" orbits to determine the error of the OPs, the residual is calculated from each subsequent tracking observation not considered in the OD. The telescope pointing errors are calculated in the along and cross track directions to give an idea of the chance of reacquiring the target. The range difference is also determined but is less important for the purposes of reacquisition. The overall OP accuracy is calculated as the RMS of these differences.

To determine the potential loss of accuracy when using only a very small fraction of each pass, the OP results from OD variants (1c) and (2c) are compared. Due to the (2c) results being accurate, OD variant (2c) is then compared with the OP results from (2a) and (2b) to determine the importance of 3D positioning in very short-arc OD. The use of TLE-generated supplemental observations is investigated in (2a) and (2b) and the optimal relative weighting factor against the angular and range observations is provided that achieves the best OP accuracy.

In the next section, the results from the OD/OP analyses are presented.

ORBIT PREDICTION RESULTS

In this section the results are presented from the OD/OP study. Initially, the 1-7 day OP results are presented for the 3D data fitting cases, followed by the 1-day OP results from fitting 2D data, and finally the 1-day OP results fitting 1D data.

3.1 OP results for very short-arc and full arc ODs fitting 3D observations

Fig. 1 shows boxplot summaries for the 1–7 day OP results from the OD variant (1c) – fitting full pass 3D observations. Similarly Fig. 2 shows the boxplots from the OD variant (2c) – fitting very short-arc 3D observations. Errors in the telescope pointing are shown in the along and cross track directions, and the range residuals determined from the ranging system observations are also provided.

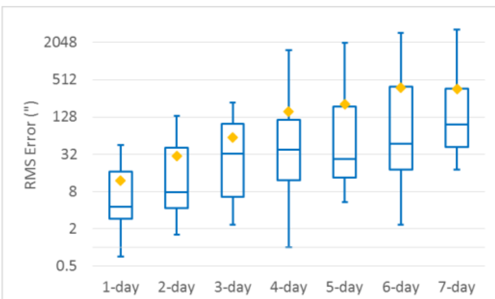

(a) Along track error

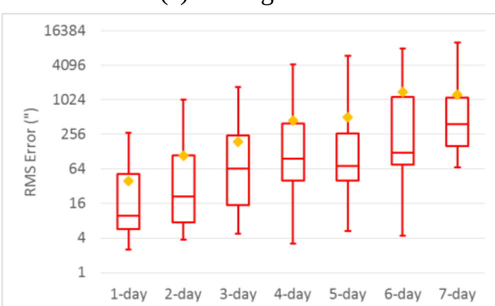

(b) Cross track error

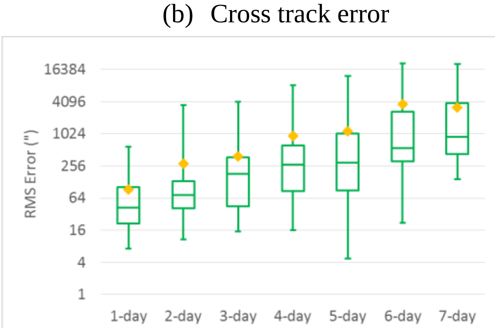

(c) Range error

Fig. 1. 1-7 day OP results fitting 3D full pass observations. Note the logarithmic scale of the error.

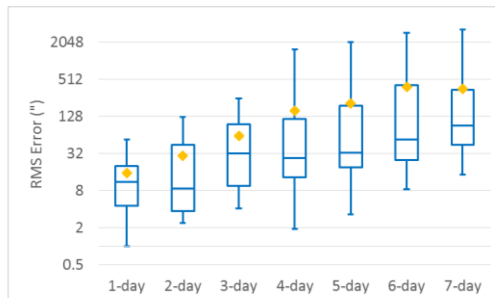

(a) Along track error

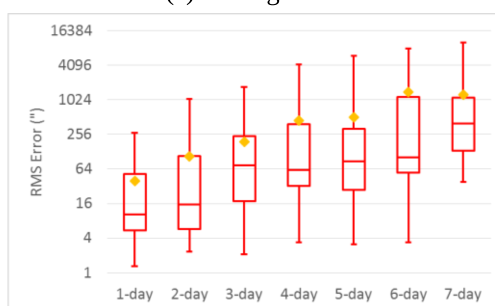

(b) Cross track error

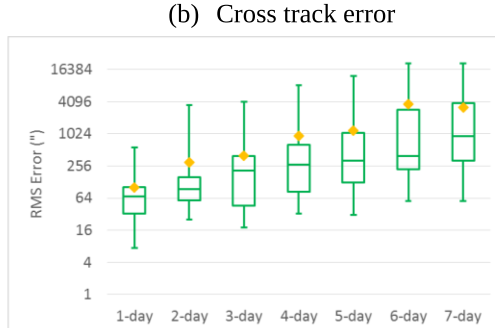

(c) Range error

Fig. 2. 1-7 day OP results fitting 3D 5 second pass observations. Note the logarithmic scale of the error.

Fig. 1 and Fig. 2 show that the loss in accuracy is not extensive considering the large reduction in observational data for the very short-arc case. Due to the 24 hour separation between the fitted passes there is not much extra information gained by considering the full pass data. As the prediction period grows, the effect of fitting the data reduces and the error is dependent on the modelling of the forces. Using full pass data gives better OP accuracy but for reacquisition in a tracking operation, short-arc data is sufficient and has a large tracking load savings.

3.2 OP results for very short-arc ODs comparing fitting 3D observations with fitting 2D observations

In this Section the OD variant (2b) is compared with (2c) to determine the range information contribution to the OP accuracy and if the same accuracy can be achieved in a purely optical tracking network.

Fig. 3. shows the results comparing the 2D case with the 3D results from the previous section for the 1-day OP errors.

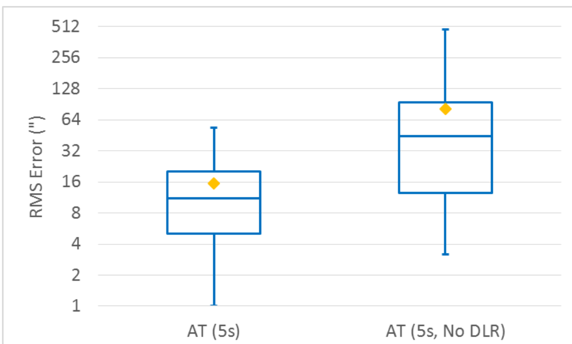

(a) Along track error

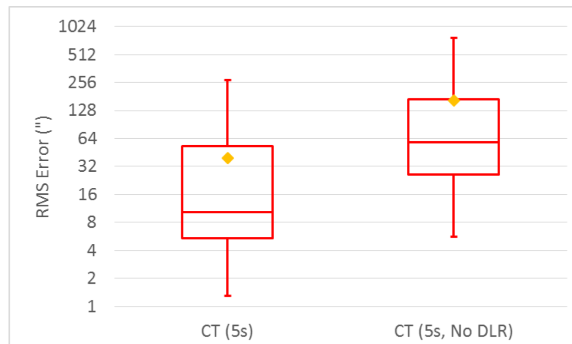

(b) Cross track error

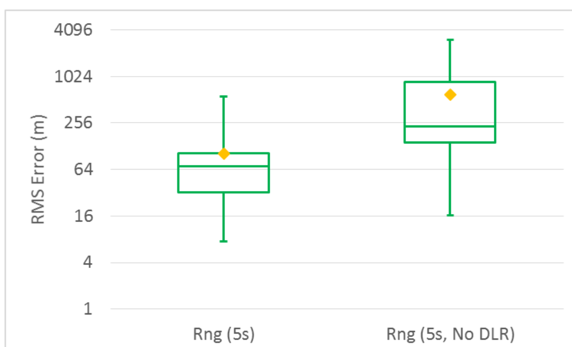

(c) Range error

Fig. 3. 1-day OP results comparing OD variants (2b) and (2c). Note the logarithmic scale of the error.

Fig. 3 shows that a purely optical system would result in much worse OPs than an optical and laser tracking system. There is a significant growth in the error in the along, cross track directions as well as the range. The 1-day OP median RMS error is approximately four times larger in the 2D short-arc fitting than the 3D short-arc fitting. Also, one of the OD cases failed to converge in the (2b) OD variant. For reliable short-arc observation fitting 3D observations are preferred.

3.2.1 Including TLE pseudo-observations to the 2D OD fitting

Including TLE pseudo-observations in OD variant (2b) improves the OP accuracy depending on the weighting factor given to the pseudo-observations relative to the angular observations. It was found that for best OP results the TLE pseudo-observations should be weighted as 10^{-16} relative to the angular observations that had unit weight. Fig. 4

shows the 1-day OP RMS errors from OD variant (2c) (fitting short-arc 3D observation passes) to OD variant (2b) (fitting short-arc 2D observation passes and optimally weighted TLE pseudo-observations).

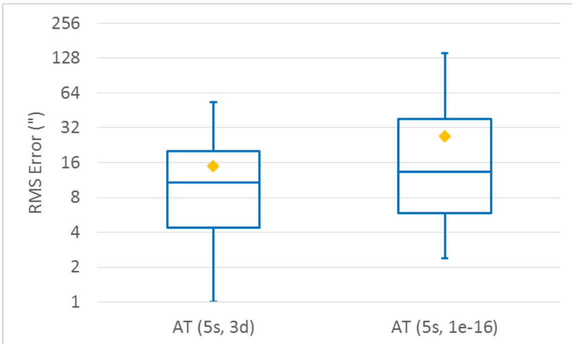

(a) Along track error

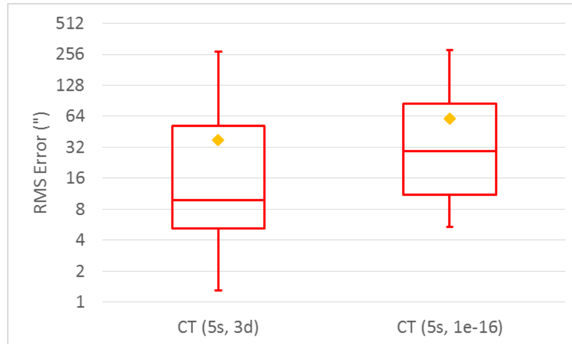

(b) Cross track error

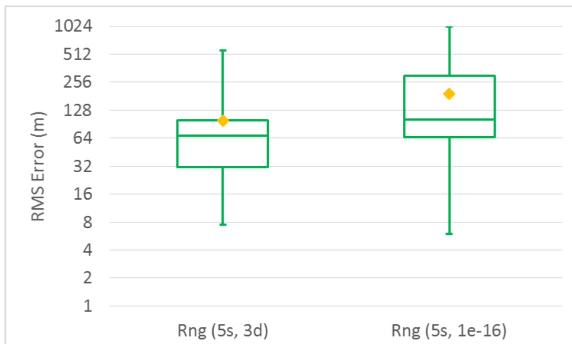

(c) Range error

Fig. 4. 1-day OP RMS error for OD variants (2c) and (2b+TLE). Note the logarithmic scale of the error.

This shows that including the optimally weighted TLE pseudo-observations improves the results significantly. The 1-day OP *averages* are now less than double the OD variant (2c) results – compared to when no pseudo-observations were included (previous section) where the average was at least 4 times greater.

3.3 OP results for very short-arc ODs comparing fitting 3D observations with fitting 1D observations

The convergence rate for OD variant (2a), i.e. fitting *only* the 1D DLR observations, was unacceptable with only 4 of the 33 1-day OP cases converging. Clearly 1D short-arc observational data is insufficient for reliable OP and other information needs to be included, such as the TLE pseudo-observations in the OD fitting.

3.3.1 Including TLE pseudo-observations to the 1D OD fitting

Including TLE pseudo-observations in OD variant (2a) improves convergence rate dramatically with 28 of the 33 1-day OP cases converging. The cases that didn't converge had no TLEs falling in the OD window. Again the OP accuracy is dependent on the weighting factor given to the pseudo-observations relative to the DLR observations. It was found that for best OP results the TLE pseudo-observations should be weighted as 10^{-6} relative to the DLR observations with unit weight. Fig. 5 shows the 1-day OP RMS errors from OD variant (2c) (fitting short-arc 3D observation passes) to OD variant (2a) (fitting short-arc 1D observation passes and optimally weighted TLE pseudo-observations).

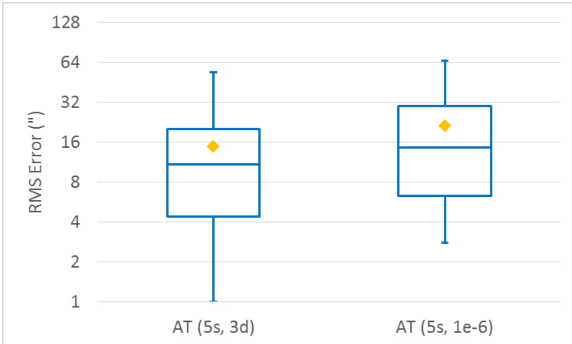

(a) Across track error

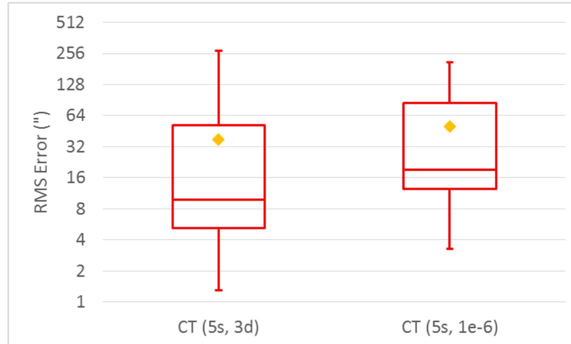

(b) Cross track error

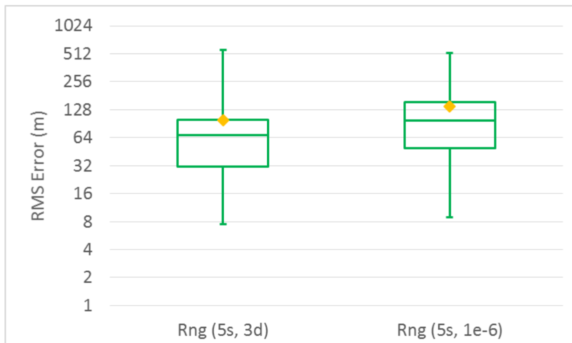

(c) Range error

Fig. 5. 1-day OP RMS error for OD variants (2c) and (2a+TLE). Note the logarithmic scale of the error.

Fig. 5. shows that including the optimally weighted TLE pseudo-observations gives good 1-day OP results from OD variant (2a) (fitting short-arc 1D observations), nearing the results from OD variant (2c). The averages are less than double the OD variant (2c) results. Overall, the 1-day OP results from OD variant (2a+TLE) are better than OD variant (2D+TLE) showing the importance of accurate range observations.

4. CONCLUSIONS

The results in this paper indicate that for short term OP, there is little extra information in the long pass data. This will result in a reduced tracking load so more objects can be routinely tracked without much loss in OP accuracy. For the cases considered, TLE pseudo-observations are very useful to improve the accuracy when fitting short-arc 2D and 1D observations – in fact it is a necessity for adequate OD convergence if considering short-arc 1D observations.

The results rely on an accurate ballistic coefficient being available, accurate tracking data, and the availability of an initial state. The other important factor is the separation time between the very short-arc observation passes. If the two 5 second passes were close to each other, then the same accuracy would not be achieved. A TLE was used for the initial state to begin the OD process, therefore the results of this paper are applicable to objects that have been previously tracked and not for catalogue build-up, i.e., the short-arc observation data is used to correct a pre-existing state. The 5 seconds of data was selected from the beginning of the passes collected to be typical of what would result from current operational practices. Future analyses will extend this method to the whole LEO region. For this to be possible an accurate estimate of the area-to-mass ratio will need to be developed similar to the ballistic coefficient estimation method [10].

The short-arc OP success is reliant on fitting 3D observational data. In a purely optical tracking scenario, the same accuracy cannot be achieved with such sparse, short-arc observations. With no angular data, i.e. fitting 1D range observations only, the OD diverges in most cases. This shows the importance of 3-dimensional positioning data. Including TLE pseudo-observations in the OD process improves the 1D and 2D results; however, it fails to reach the accuracy of the 3D fitting even with optimally weighted TLE pseudo-observations.

Future research will investigate a taxonomy for debris objects that fuses all possible data from multiple tracking sensors to create a realistic representation of each object. The assumption of spherical objects will be relaxed. Ideally, the object characterisation should be dynamic and be a feature in the catalogue. This will be part of the focus of future studies to improve debris OP.

ACKNOWLEDGEMENT

The authors would like to gratefully acknowledge the Australian Research Council's research grant support for this project through the Linkage Projects scheme (LP130100243).

REFERENCES

1. Sang, J. and C. Smith, *An analysis of observations from EOS Space Debris Tracking System*, in *11th Australian Space Science Conference*, I. Cairns and W. Short, Editors. 2011: Canberra, Australia. p. 179-189.
2. Sang, J. and C. Smith, *Performance Assessment of the EOS Space Debris Tracking System*, in *2012 AIAA/AAS Astrodynamics Specialist Conference*. 2012: Minneapolis, MN.
3. Bennett, J.C., J. Sang, C.H. Smith, and K. Zhang, *Accurate orbit predictions for debris orbit manoeuvre using ground-based lasers.* Adv. Space Res., 2013. **52**(11): p. 1876-1887.
4. Sang, J. and J.C. Bennett, *Achievable debris orbit prediction accuracy using laser ranging data from a single station.* Advances in Space Research, 2014. **54**(1): p. 119-124.
5. Sang, J., J.C. Bennett, and C. Smith, *Experimental results of debris orbit predictions using sparse tracking data from Mt. Stromlo.* Acta Astronautica, 2014. **102**(0): p. 258-268.
6. Sang, J., I. Ritchie, M. Pearson, and C. Smith, *Results and analysis of debris tracking from Mt Stromlo*, in *2013 AMOS Space Surveillance Technologies Conference*. 2013: Maui, Hawaii.
7. Förste, C., et al., *EIGEN-GL05C - A new global combined high-resolution GRACE-based gravity field model of the GFZ-GRGS cooperation.* Geophys. Res. Abstr., 2008. **10, EGU2008-A-03426**.
8. Eanes, R.J. and S. Bettadpur, *The CSR 3.0 global ocean tide model: diurnal and semi-diurnal ocean tides from TOPEX/Poseidon altimetry*, in *Technical Memorandum*. 1995, Center for Space Research.
9. McCarthy, D.D. and G.e. Petit, *IERS Conventions (2003)*, in *IERS Technical Note 32*. 2004, Frankfurt am Main: Verlag des Bundesamts für Kartographie und Geodäsie.
10. Sang, J., J.C. Bennett, and C.H. Smith, *Estimation of ballistic coefficients of low altitude debris objects from historical two line elements.* Adv. Space Res., 2013. **52**(1): p. 117-124.
11. Picone, J.M., A.E. Hedin, D.P. Drob, and A.C. Aikin, *NRLMSISE-00 empirical model of the atmosphere: Statistical comparisons and scientific issues.* Journal of Geophysical Research: Space Physics, 2002. **107**(A12): p. 1468.
12. Vallado, D.A., P. Crawford, R. Hujsak, and T.S. Kelso. *Revisiting Spacetrack Report #3*. in *AIAA*. 2006.